Published in final edited form as:
*J Tissue Eng Regen Med*. 2013 October ; 7(10): 777–787. doi:10.1002/term.1466.

# Novel non-rigid calcium phosphate scaffold seeded with umbilical cord stem cells for bone tissue engineering

**WahWah Thein-Han**[1], **Michael D. Weir**[1], **Carl G. Simon**[2], and **Hockin H. K. Xu**[1,3,*]

[1]Biomaterials & Tissue Engineering Division, Department of Endodontics, Prosthodontics and Operative Dentistry, University of Maryland Dental School, Baltimore, MD 21201

[2]Biomaterials Group, National Institute of Standards and Technology (NIST) Gaithersburg, MD 20899

[3]Center for Stem Cell Biology & Regenerative Medicine, University of Maryland School of Medicine, Baltimore, MD 21201, USA

## Abstract

The need for bone repair has increased as the population ages. Non-rigid calcium phosphate scaffolds could provide compliance for micro-motions within the tissues and yet have load-supporting strength. The objectives of this study were to (1) develop a non-rigid calcium phosphate cement (CPC) scaffold; and (2) investigate human umbilical cord mesenchymal stem cell (hUCMSC) proliferation, osteodifferentiation and mineralization on non-rigid CPC for the first time. Non-rigid CPC was fabricated by adding extra tetracalcium phosphate in the traditional CPC, and by incorporating chitosan, absorbable fibers, and hydrogel microbeads. The non-rigid CPCmicrobead scaffold possessed a strain-at-failure of 10.7%, much higher than the traditional CPC's strain of 0.05% which is typical for brittle bioceramics. Flexural strength of non-rigid CPCmicrobead was 4-fold that of rigid CPC-mircobead scaffold, while work-of-fracture (toughness) was increased by 20-fold. The strength of non-rigid CPC-microbead-fiber scaffold matched that of cancellous bone. hUCMSCs on non-rigid CPC proliferated from 100 cells/mm$^2$ at 1 day, to 600 cells/mm$^2$ at 8 days. Alkaline phosphatase, osteocalcin, and collagen gene expressions of hUCMSCs were greatly increased, and the cells synthesized bone minerals. hUCMSCs on non-rigid CPC-microbead-fiber construct had higher bone markers and more mineralization than those on rigid CPC. In conclusion, this study developed the first non-rigid, *in situ*-setting calcium phosphate-microbead-fiber scaffold with a strain-at-failure exceeding 10%. hUCMSCs showed excellent proliferation, osteodifferentiation, and mineralization on non-rigid CPC scaffold. The novel non-rigid CPC-hUCMSC construct with good strength, high strain-at-failure and toughness, as well as superior cell proliferation, osteodifferentiation and mineralization is promising for load-bearing bone regeneration applications.

### Keywords

Calcium phosphate cement (CPC); non-rigid scaffold; strength and strain; human umbilical cord stem cells; osteogenic differentiation; bone tissue engineering

[*]Corresponding author: Hockin Xu, Professor, Director of Biomaterials & Tissue Engineering Division, University of Maryland Dental School, 650 West Baltimore Street, Baltimore, MD 21201, Ph: 410-706-7047. Fax: 410-706-2089. hxu@umaryland.edu.

## 1. Introduction

Seven million people suffer bone fractures each year in the U.S., and musculoskeletal conditions cost $215 billion annually (Praemer *et al.*, 1999). These numbers are increasing rapidly due to an aging population (Laurencin *et al.*, 1999; Johnson *et al.*, 2007; Mao *et al.*, 2007; Atala, 2009). Tissue engineering approaches are being developed to meet this need (Gomes *et al.*, 2004; Jansen *et al.*, 2005; Mikos *et al.*, 2006; Discher *et al.*, 2009; Aoki *et al.*, 2010; Varghese *et al.*, 2010). Human bone marrow-derived mesenchymal stem cells (hBMSCs) were frequently investigated for tissue engineering therapies (Nuttelman *et al.*, 2004; Yao *et al.*, 2005; Benoit *et al.*, 2006; Mao *et al.*, 2006; Salinas and Anseth, 2008; Sundelacruz and Kaplan, 2009). Recently, human umbilical cord mesenchymal stem cells (hUCMSCs) were differentiate into adipocytes, osteoblasts, chondrocytes, neurons, and endothelial cells (Wang *et al.*, 2004; Baksh *et al.*, 2007; Bailey *et al.*, 2007; Jäger *et al.*, 2007; Wang *et al.*, 2009). Umbilical cords are inexhaustible and inexpensive, and hUCMSCs can be harvested without an invasive procedure. hUCMSCs appeared to be a primitive MSC population that expressed certain human embryonic stem cell markers and exhibited high plasticity and developmental flexibility, with no immunorejection in pilot animal studies (Weiss *et al.*, 2006; Can and Karahuseyinoglu, 2007).

Engineered scaffolds serve as a matrix for cell function while maintaining the volume and supporting the external stresses. Due to their similarity to apatite minerals in natural bone, calcium phosphate (CaP) bioceramics such as hydroxyapatite (HA) are important for bone repair (Ducheyne and Qiu, 1999; Foppiano *et al.*, 2004; Radin *et al.*, 2005). CaP implants provide an ideal environment for cellular reaction and colonization by osteoblasts, thus forming a functional interface *in vivo* (Leach *et al.*, 2006; Reilly *et al.*, 2007). For preformed bioceramic scaffolds to fit in a bone cavity, the surgeon needs to machine the graft or carve the surgical site, leading to increases in bone loss, trauma, and surgical time (Laurencin *et al.*, 1999). In contrast, calcium phosphate cements can be injected and set *in situ* to provide intimate adaptation to complex-shaped defects. The first calcium phosphate cement (CPC) was developed in 1986 (Brown and Chow, 1986). Since then, other novel formulations were developed (Barralet *et al.*, 2002; Bohner and Baroud, 2005; Link *et al.*, 2008; Xu *et al.*, 2008). CPC was approved in 1996 by the Food and Drug Administration (FDA) for repairing craniofacial defects (Friedman *et al.*, 1998). However, due to its brittleness, CPC is "limited to the reconstruction of non-stress-bearing bone" (Shindo *et al.*, 1993; Friedman *et al.*, 1998). Recently, absorbable fibers and chitosan were used to improve the load-bearing capability of CPC and to create macroporous scaffolds (Xu *et al.*, 2004, 2007).

It is desirable to develop a non-rigid and tough CPC scaffold, which could be used in periodontal bone repair, spinal fusion and other applications where load and micro-motions need to be tolerated. For example, when the traditional CPC was used in periodontal bone repair, tooth mobility resulted in the early displacement and failure of the brittle implants (Brown *et al.*, 1998). A non-rigid CPC would be useful to provide the needed compliance for tooth motion without fracturing the implant. Chitosan and its derivatives are biodegradable and osteoconductive, and are good candidates for the elastomeric matrix (Muzzarelli *et al.*, 1993). In a recent study, a non-rigid CPC was developed by adding tetracalcium phosphate to the CPC powder and chitosan to the CPC liquid (Xu *et al.*, 2006). However, while hydrogel microbeads and fibers were incorporated into the regular CPC (Zhao *et al.*, 2010a), the previous non-rigid CPC had no hydrogel microbeads nor fiber reinforcement. In addition, stem cells have not been seeded on the non-rigid CPC.

Therefore, the objectives of this study were to incorporate fibers and hydrogel microbeads into the non-rigid CPC, and to investigate hUCMSC seeding on the non-rigid CPC for the first time. It was hypothesized that: (1) While the CPC composite scaffold would be weak

mechanically, adding chitosan and fibers would greatly increase its strain-at-failure and strength; (2) hUCMSCs on the non-rigid CPC composite would have good viability and proliferation rate; (3) Non-rigid CPC composite would support hUCMSC differentiation, and adding chitosan and fibers would enhance the bone marker gene expressions and bone mineral synthesis by the hUCMSCs.

## 2. MATERIALS AND METHODS

### 2.1. Calcium phosphate powder and liquid

CPC powder consisted of a mixture of tetracalcium phosphate (TTCP) ($Ca_4[PO_4]_2O$) and dicalcium phosphate anhydrous (DCPA) ($CaHPO_4$). TTCP was synthesized from a solid-state reaction between equimolar amount of DCPA and calcium carbonate (J.T. Baker, Philipsburg, NJ). The mixture was heated to 1500 °C and then ground and sieved, yielding TTCP particles of 1 to 80 μm, with a median of 17 μm. DCPA was ground to obtain a median particle size of 1 μm.

Two types of CPC powders were prepared. The first consisted of a mixture at a TTCP:DCPA molar ratio of 1 to 1. The CPC liquid was distilled water. This TTCP:DCPA ratio was the same as that of the traditional CPC (Friedman *et al.*, 1998; Zhao *et al.*, 2010a), and it is hereinafter referred to as “rigid CPC”.

The second CPC powder had a TTCP:DCPA ratio of 3.7 to 1, following a previous study on formulating a non-rigid CPC (Xu *et al.*, 2006). The higher TTCP content was shown to facilitate the gelling of chitosan, yielding a CPC-chitosan composite with a high ductility (Xu *et al.*, 2006). The CPC liquid consisted of chitosan lactate (VANSON, Redmond, WA) dissolved in water, at a chitosan/(chitosan + water) mass fraction = 15% (Xu *et al.*, 2006).

### 2.2. Calcium phosphate-hydrogel microbead composite

The previous non-rigid CPC did not contain hydrogel microbeads or absorbable fibers for reinforcement (Xu *et al.*, 2006). It is desirable to include hydrogel microbeads in CPC to potentially deliver growth factors, and then for the microbeads to degrade and form macropores in CPC. The present study focused on the effect of microbeads and fibers on the mechanical properties of the non-rigid CPC, as well as the seeding of hUCMSCs for osteogenic differentiation. A future study will investigate the delivery of various growth factors in the microbeads in CPC. To make the microbeads, a sodium alginate solution (1.2% mass fraction) was prepared by dissolving 0.3 g alginate (ProNova, Oslo, Norway) in 25 mL of 155 mM sodium chloride (Zhao *et al.*, 2010a). The alginate solution was sprayed from a syringe into a 100 mM calcium chloride solution, where gelation occurred upon contact. The syringe was connected to a bead generation device (Nisco, Zurich, Switzerland) (Zhao *et al.*, 2010a). Nitrogen gas at a pressure of 10 psi was fed to the gas inlet to form a coaxial air flow with which to break up the alginate into fine droplets. The microbeads thus fabricated had a mean diameter of 207 μm, suitable for forming an injectable CPC-microbead paste and macropore formation in CPC (Zhao *et al.*, 2010a).

Three groups of specimens were made. Group 1 had two materials: Rigid CPC-microbead scaffold which served as control; and non-rigid CPC-microbead scaffold. Each aforementioned CPC powder was mixed with the liquid at a powder:liquid mass ratio of 2:1 to form a paste. Microbeads were mixed with the paste, at a microbead volume/specimen volume fraction of 50%. The paste was placed into a rectangular mold of 3 × 4 × 25 mm, incubated in a humidor at 37 °C for 4 h, then immersed in a simulated physiological solution (1.15 mmol/L Ca, 1.2 mmol/L P, 133 mmol/L NaCl, 50 mmol/L Hepes, buffered to a pH 7.4) at 37 °C for 20 h.

The purpose of group 2 was to investigate the effect of fiber reinforcement on mechanical properties. A resorbable suture fiber (Vicryl, polyglactin 910, Ethicon, NJ) at a 3-mm length was used, because this fiber had a high strength, provided reinforcement for about four weeks, and then dissolved and formed macropores in CPC (Xu *et al.*, 2004). The fibers were mixed with the nonrigid CPC and microbead paste, at fiber volume fractions (fiber volume/specimen volume) of: 0%, 10%, 20%, 30%, and 40%. Fibers of more than 40% were not used in order to obtain a flowable CPC paste. Specimens were fabricated in the same manner as described for the first group.

The purpose of group 3 was to investigate hUCMSC seeding on non-rigid CPC. Three materials were tested: Rigid CPC control; non-rigid CPC-microbead scaffold; and non-rigid CPC-microbead-fiber scaffold. The fiber volume fraction was 40%. Disk specimens of 12-mm diameter and 2-mm thickness were fabricated for the cell experiments.

### 2.3. Mechanical testing

A three-point flexural test was used with a span of 20 mm at a crosshead speed of 1 mm/min on a computer-controlled Universal Testing Machine (MTS, Eden Prairie, MN). Flexural strength, work-of-fracture, elastic modulus, and strain-at-failure were measured. The work-of-fracture (toughness) is a measurement of the energy required to fracture the specimen, calculated as the area under the load-displacement curve divided by the specimen's cross-sectional area (Xu *et al.*, 2007).

### 2.4. hUCMSC attachment, proliferation, and viability

hUCMSCs were obtained commercially (ScienCell, Carlsbad, CA), which were derived from umbilical cords of healthy babies and harvested using established methods (Wang *et al.*, 2004; Bailey *et al.*, 2007). The use of hUCMSCs was approved by the University of Maryland. Cells were cultured in a low-glucose Dulbecco's modified Eagle's medium (DMEM), supplemented with 10% fetal bovine serum (FBS) and 1% penicillin-streptomycin (10,000 IU-10,000 μg/ml) (Invitrogen, Carlsbad, CA) (control media). At 80–90% confluence, hUCMSCs were detached by trypsin. Passage 4 cells were used. The osteogenic media contained 100 nM dexamethasone, 10 mM β-glycerophosphate, 0.05 mM ascorbic acid, and 10 nM 1α,25-Dihydroxyvitamin (Sigma) (Wang *et al.*, 2009; Zhao *et al.*, 2010a). A cell suspension of 150,000 cells in 2 mL of osteogenic media was added to each well containing a CPC disk. The media was changed every 2 d.

At 1, 4, and 8 d, the cells were stained with a live/dead kit (Invitrogen) and viewed by epifluorescence microscopy (TE2000S, Nikon, Melville, NY). Three randomly-chosen fields of view were photographed from each disk. Five disks yielded 15 photos for each material. The cells were counted. $N_{Live}$ is the number of live cells. $N_{Dead}$ is the number of dead cells. The percentage of live cells, $P = N_{Live}/(N_{Live} + N_{Dead})$. Live cell density, D, is the number of live cells attached to the specimen divided by the surface area, A: $D = N_{Live}/A$ (Zhao *et al.*, 2010b).

hUCMSCs were seeded on the scaffolds and cultured for 1 and 4 d. They were fixed with 2.5% glutaraldehyde in 0.1 M cacodylate buffer pH 7.4, dehydrated with a graded series of ethanol (25–100%), rinsed with hexamethyldisilazane, and sputter-coated with gold. They were then examined using a scanning electron microscope (SEM, JEOL 5300, Peabody, MA).

### 2.5. Immunofluorescence of actin fibers in hUCMSCs attached on scaffolds

Actin stress fibers inside the cells are related to the initial cell attachment. hUCMSC constructs after 1 d culture were washed with PBS, fixed with 4% parformaldehyde for 20

min, permeabilized with 0.1% Triton X-100 for 5 min, and blocked with 0.1% bovine serum albumin (BSA) for 30 min. An actin cytoskeleton and focal adhesion staining kit (Chemicon, Temecula, CA) was used following the manufacturer's instructions, which stained actin fibers into a red color. Fluorescence microscopy (TE2000S, Nikon) was used to examine the specimens. The actin fluorescence intensity was increased when the actins stress fiber density increased. The fluorescence intensity of actin fibers in hUCMSCs was measured via a NIS-Elements BR software (Nikon).

### 2.6. hUCMSC osteogenic differentiation

Quantitative real-time reverse transcription polymerase chain reaction measurement (qRT-PCR, 7900HT, Applied Biosystems, Foster City, CA) was used. Each well with a CPC disk was seeded with 150,000 cells and cultured in osteogenic media for 1, 4, and 8 d (Kim *et al.*, 2009). The total cellular RNA on the scaffolds were extracted with TRIzol reagent (Invitrogen) and reverse-transcribed into cDNA. TaqMan gene expression kits were used to measure the transcript levels of the proposed genes on human alkaline phosphatase (ALP, Hs00758162_m1), osteocalcin (OC, Hs00609452_g1), collagen type I (Coll I, Hs00164004), and glyceraldehyde 3-phosphate dehydrogenase (GAPDH, Hs99999905). Relative expression for each target gene was evaluated using the $2^{-\Delta\Delta Ct}$ method (Livak and Schmittgen, 2001). Ct values of target genes were normalized by the Ct of the TaqMan human housekeeping gene GAPDH to obtain ΔCt. These values were then subtracted by the Ct value of the hUCMSCs cultured on tissue culture polystyrene in the control media for 1 d (the calibrator) to obtain the ΔΔCt values (Kim *et al.*, 2009).

### 2.7. hUCMSC mineralization

First, hUCMSCs were seeded on tissue culture polystyrene (TCPS), and cultured in control media or osteogenic media for 14 d. Alizarin Red S (ARS) staining was used to examine bone mineralization. Specimens were washed with PBS, fixed with 10% formaldehyde, and stained with ARS (Millipore, Billerica, MA), which stained calcium minerals into a red color. The purpose of this was to confirm that hUCMSCs cultured in osteogenic media could synthesize minerals.

Second, hUCMSCs were seeded on three scaffolds: Rigid CPC; non-rigid CPC-microbead scaffold; and non-rigid CPC-microbead-fiber scaffold. The cells on CPC disks were cultured in osteogenic media for 14 d and then stained with ARS. An osteogenesis assay (Millipore, Billerica, MA) was used to measure the mineral concentration following the manufacture's instructions. CPC without hUCMSC seeding was used as control. The control's Alizarin Red concentration was subtracted from the Alizarin Red concentration of the corresponding scaffold with hUCMSCs, to yield the net mineral concentration synthesized by the cells.

One-way and two-way ANOVA were performed to detect significant effects of the variables. Tukey's multiple comparison tests were done to compare the data at $p$ of 0.05.

## 3. RESULTS

Fig. 1 shows the difference between traditional rigid CPC and the new non-rigid CPC scaffolds. In (A), the rigid CPC-mircobead specimen fractured catastrophically. In (B), the non-rigid CPCmicrobead specimen could be bent without fracture. In (C), the rigid CPC-mircobead specimens fractured at a displacement of about 0.1 mm, while the non-rigid CPC-microbead specimens reached a displacement of 3 mm before fracture. In (D), flexural strength of the non-rigid CPCmicrobead specimens was 4-fold higher than that of rigid CPC-mircobead specimens ($p < 0.05$). In (E), work-of-fracture was increased from 5 J/m$^2$ for rigid CPC-mircobead to 123 J/m$^2$ for non-rigid CPC-microbead scaffold ($p < 0.05$). In

(F), elastic moduli were not significantly different ($p > 0.1$). In (G), the strain-at-failure for the non-rigid CPC-microbead scaffold reached 10.7%, much higher than the 0.05% of the rigid CPC-mircobead specimens ($p < 0.05$).

Fig. 2 plots the effect of fiber volume fraction on mechanical properties of non-rigid CPC-microbead scaffold. In (A), the load-bearing capability was increased with higher fiber content. In (B), flexural strength increased with fiber content, reaching (3.8 ± 1.1) MPa at 40% fibers. Work-of-fracture was also increased by about 5-fold. Elastic modulus increased but not significantly ($p > 0.1$), likely because the fibers were flexible and not stiff.

In Fig. 3, live cells were stained green and were numerous on all materials at 1 d (A–C). Cells proliferated well, with many more cells at 8 d (D–F). Dead cells were stained red and were very few. In (G), the percentage of live cells was above 90% for all constructs. In (H), the live cell density was increased from about 100 cells/mm$^2$ at 1 d, to 600 cells/mm$^2$ at 8 d ($p < 0.05$).

Fig. 4 shows the fluorescence results of actin stress fibers. Compared to the rigid CPC in (A), the red fluorescence intensified in (B) the non-rigid CPC-microbead, and (C) the non-rigid CPC-microbead-fiber scaffold. This indicates an increased number of actin stress fibers in the hUCMSCs. The higher magnification in (D) shows numerous actin stress fibers. In (E), the actin fiber fluorescence intensity, proportional to the amount of actin fibers, increased from rigid CPC to non-rigid CPC-microbead, and to non-rigid CPC-microbead-fiber scaffold ($p < 0.05$).

Examples of hUCMSC attachment on the scaffolds are shown in Fig. 5. In (A), after 1 d, the cells attached and spread well on rigid CPC. In (B) and (C), cells attached to non-rigid CPC-microbead- fiber construct. “C” refers to the hUCMSCs, with cytoplasmic extensions “E” that anchored to the fibers “F”. In (D), the cells anchored to the nano-sized apatite crystals in the CPC matrix. The hUCMSCs had attained a normal polygonal morphology.

The osteogenic differentiation results are plotted in Fig. 6. In (A), the ALP gene expression was minimal at 1 d, greatly increased at 4 d, then slightly decreased at 8 d. At 4 d, the hUCMSCs of the non-rigid CPC-microbead-fiber construct had the highest ALP peak, followed by that of nonrigid CPC construct, and then followed by rigid CPC; these three values were significantly different from each other ($p < 0.05$). In (B), OC peaked at 8 d. At 8 d, the OC values of non-rigid CPC-microbead-fiber and the non-rigid CPC constructs were similar; both were higher than that of rigid CPC ($p < 0.05$). In (C), the collagen I gene expression showed a similar trend as that of OC.

ARS stained calcium minerals into a red color. In Fig. 7A, hUCMSCs were cultured in control media, and no red staining was found. In Fig. 7B, hUCMSCs on TCPS in osteogenic media showed significant mineral staining. In (C), ARS staining yielded a red color for the CPC disk with no cells, because CPC consisted of hydrxyapatite minerals. When hUCMSCs were seeded on (D) rigid CPC, (E) non-rigid CPC-microbead scaffold, and (F) non-rigid CPC-microbead-fiber scaffold, the red staining became progressively thicker and darker than that of CPC disk without cells. There was a layer of new mineral matrix synthesized by the cells covering the disks. The thick matrix mineralization formed in the cell-scaffold construct covered not only the top surface, but also the peripheral areas at the sides of the disk. The data from the osteogenesis assay is plotted in (G). The mineral synthesized by the hUCMSCs on the non-rigid CPC-microbead-fiber scaffold was significantly more than those of the other two constructs ($p < 0.05$).

## 4. DISCUSSION

Calcium phosphate bioceramics are bioactive and osteoconductive. However, bioceramics are brittle and can fracture catastrophically at a small deformation strain. The present study developed the first non-rigid CPC-hydrogel microbead scaffold with a large strain-at-failure of 10.7%. In contrast, traditional CPC had a strain-at-failure of only 0.05%, which is typical for brittle bioceramics. A non-rigid, injectable CPC could provide compliance for micro-motions within the tissue without fracture, useful for periodontal bone repair, spinal fusion, and other orthopedic applications that require stress and micro-motion capabilities. In a previous study (Xu *et al.*, 2006), a non-rigid CPC was formulated but it did not contain hydrogel microbeads or fiber reinforcement, and there was no study on stem cell seeding on non-rigid CPC. In the present study, the addition of fibers increased the strength of the non-rigid CPC containing hydrogel microbeads. Its strength of 4 MPa approached the reported tensile strength of 3.5 MPa for cancellous bone (Damien and Parsons, 1990). Literature search indicated that this is the first calcium phosphate-hydrogel microbead scaffold with a strain exceeding 10% and a strength matching that of cancellous bone.

Previous studies have developed injectable polymeric scaffolds for cell delivery. An injectable polymeric carrier for cell delivery had a compressive strength of about 0.7 MPa and an elastic modulus of 0.008 GPa (Shi *et al.*, 2007). Hygrogels for cell delivery had a tensile strength of about 0.07 MPa and a modulus of 0.0001 GPa (Kuo and Ma, 2001; Drury *et al.*, 2004). These materials are meritorious for tissue engineering. However, it was correctly concluded that “Hydrogel scaffolds are used in nonload bearing bone tissue engineering. … They do not possess the mechanical strength to be used in load bearing applications” (Drury *et al.*, 2004). In the present study, the non-rigid CPC construct is substantially stronger mechanically, and may be useful for stem cell delivery in a wide range of load-bearing maxillofacial and orthopedic applications.

While hBMSCs are an important for bone regeneration, their limitations include donor site morbidity and lower self-renewal and differentiation potential with aging. Recent studies demonstrated the promise of hUCMSCs, in which cells were cultured with tissue culture plastic, polymer scaffolds, and calcium phosphate scaffolds (Wang *et al.*, 2004; Baksh *et al.*, 2007; Wang *et al.*, 2009; Zhao *et al.*, 2010b). The present study investigated hUCMSC seeding on the new nonrigid CPC for the first time. hUCMSCs were able to adhere, spread and remain viable on the nonrigid CPC. hUCMSCs anchored to the nano-sized apatite crystals and fibers in the non-rigid scaffold. Cells proliferated rapidly with the number increasing by 6-fold in 7 d. The immunofluorescence experiment showed that actin stress fibers were numerous in the hUCMSCs attaching to the CPC-based scaffolds. These actin stress fibers anchor to the cell membrane at locations that are frequently connected to the extracellular matrix or the scaffold substrate. The fluorescence intensity of the actin stress fibers of hUCMSCs on the non-rigid CPC-microbead-fiber scaffold was nearly 2-fold that on the traditional rigid CPC. The hUCMSCs differentiated into the osteogenic lineage. Previous studies showed that ALP, OC, and collagen I gene expressions played key roles in the osteogenic differentiation of MSCs (Datta *et al.*, 2004; Lavery *et al.*, 2009). The present study showed that these osteogenic markers were highly expressed by the hUCMSCs on the non-rigid CPC. ALP is an enzyme expressed by MSCs during osteogenesis and is a well-defined marker for their differentiation (Leach *et al.*, 2006; Reilly *et al.*, 2007). Previous studies showed that the ALP gene expression was low at 1 d, peaked at 4 d, and then decreased at 8 d (Kim *et al.*, 2009). The OC expression showed a high peak at 8 d, which was slightly later than ALP peak at 4 d (Kim *et al.*, 2009). Our results for the hUCMSCs on the non-rigid CPC constructs are consistent with these previous findings.

The fiber-containing non-rigid construct had higher ALP expression at 4 d than those on the traditional rigid CPC without fibers. The OC and collagen I expressions of hUCMSCs were also higher for the non-rigid CPC with fibers than those for the rigid CPC without fibers. The suture fiber used in the non-rigid construct consisted of individual fibers braided to form a bundle. The individual fiber diameter was about 14 μm. The bundle had a diameter of about 300 μm with a rough surface. The rough surface of the non-rigid CPC-microbead-fiber construct likely facilitated the hUCMSC attachment and osteogenic differentiation. A previous study showed a 3-fold greater bone tissue ingrowth in defects containing carbon-nanotube nanocomposite scaffold, compared to control polymer scaffolds without nanotubes (Sitharaman *et al.*, 2008). This large increase was attributed to the high surface area and roughness, which may have enhanced cell attachment and stimulated the cells to synthesize the extracellular matrix (Sitharaman *et al.*, 2008). Furthermore, the non-rigid CPC without fibers had higher ALP, OC and collagen I expressions than the traditional rigid CPC. Hence, it is possible that the incorporation of chitosan, which the rigid CPC did not contain, may have also contributed to the osteodifferentiation of the cells (Thein-Han *et al.*, 2009). The ARS mineral staining became a darker and thicker red when the non-rigid CPC contained fibers, compared to that without fibers. The hUCMSCs of the non-rigid CPC-microbead-fiber scaffold synthesized much more bone minerals than that of the rigid CPC. These results indicate that the novel non-rigid CPC-microbead-fiber scaffold seeded with hUCMSCs may be a promising construct for bone tissue engineering applications. Further animal studies are needed to investigate its bone regeneration efficacy *in vivo*.

## 5. CONCLUSIONS

This study developed a novel non-rigid CPC-hydrogel-fiber-hUCMSC construct, and investigated hUCMSC proliferation, osteodifferentiation and mineral synthesis on the non-rigid CPC for the first time. The non-rigid scaffold had a strain-at-failure that exceeded 10%; in contrast, traditional rigid CPC fractured catastrophically at a strain of 0.05%, which is typical for brittle bioceramics. The strength of the non-rigid scaffold matched that of cancellous bone. The non-rigid CPC construct is promising to provide compliance for micro-motions within the tissues and yet have load-supporting strength, which may be suitable for periodontal bone repair, alveolar bone augmentation, spinal fusion, and other load-bearing repairs. hUCMSCs proliferated rapidly on non-rigid CPC, increasing by 6-fold in a week. hUCMSCs on non-rigid CPC-microbead-fiber construct had higher ALP, OC and collagen I expressions than those on traditional rigid CPC. hUCMSCs synthesized much more bone minerals on the non-rigid CPC-microbead-fiber scaffold than on the rigid CPC. Therefore, the non-rigid, tough and strong CPC-hUCMSC construct with excellent cell proliferation, osteogenic differentiation and mineral synthesis is promising for bone tissue engineering applications.

## Acknowledgments

We thank Dr. L. C. Chow and Dr. S. Takagi at the Paffenbarger Research Center and Dr. Liang Zhao at the University of Maryland Dental School for discussions and help. This study was supported by NIH grants R01 DE14190 and R01 DE17974 (HX), Maryland Stem Cell Research Fund grant 2008-MSCRFE-0109-00 (HX), the University of Maryland Dental School, and the United States National Institute of Standards and Technology (NIST).

## References

Aoki T, Ohnishi H, Oda Y, Tadokoro M, Sasao M, Kato H, Hattori K, Ohgushi H. Generation of induced pluripotent stem cells from human adipose-derived stem cells without c-MYC. Tissue Eng A. 2010; 16:2197–2206.

Atala A. Engineering organs. Curr Opin Biotechnol. 2009; 20:575–592. [PubMed: 19896823]

Baksh D, Yao R, Tuan RS. Comparison of proliferative and multilineage differentiation potential of human mesenchymal stem cells derived from umbilical cord and bone marrow. Stem Cells. 2007; 25:1384–1392. [PubMed: 17332507]

Bailey MM, Wang L, Bode CJ, Mitchell KE, Detamore MS. A comparison of human umbilical cord matrix stem cells and temporomandibular joint condylar chondrocytes for tissue engineering temporomandibular joint condylar cartilage. Tissue Eng. 2007; 13:2003–2010. [PubMed: 17518722]

Barralet JE, Gaunt T, Wright AJ, Gibson IR, Knowles JC. Effect of porosity reduction by compaction on compressive strength and microstructure of calcium phosphate cement. J Biomed Mater Res B. 2002; 63:1–9.

Benoit DSW, Nuttelman CR, Collins SD, Anseth KS. Synthesis and characterization of a fluvastatin-releasing hydrogel delivery system to modulate hMSC differentiation and function for bone regeneration. Biomaterials. 2006; 27:6102–6110. [PubMed: 16860387]

Bohner M, Baroud G. Injectability of calcium phosphate pastes. Biomaterials. 2005; 26:1553–1563. [PubMed: 15522757]

Brown GD, Mealey BL, Nummikoski PV, Bifano SL, Waldrop TC. Hydroxyapatite cement implant for regeneration of periodontal osseous defects in humans. J Periodont. 1998; 69:46–157.

Brown, WE.; Chow, LC. 'A New Calcium Phosphate Water Setting Cement'. In: Brown, PW., editor. Cements Research Progress. Westerville, OH, USA: Am Ceram Soc; 1986. p. 352-379.

Can A, Karahuseyinoglu S. Concise review: human umbilical cord stroma with regard to the source of fetus-derived stem cells. Stem Cells. 2007; 25:2886–2895. [PubMed: 17690177]

Damien CJ, Parsons JR. Bone graft and bone graft substitutes: a review of current technology and applications. J Appl Biomater. 1990; 2:187–208. [PubMed: 10149083]

Datta N, Holtorf HL, Sikavitsas VI, Jansen JA, Mikos AG. Effect of bone extracellular matrix synthesized in vitro on the osteoblastic differentiation of marrow stromal cells. Biomaterials. 2005; 26:971–977. [PubMed: 15369685]

Discher DE, Mooney DJ, Zandstra PW. Growth factors, matrices, and forces combine and control stem cells. Science. 2009; 324:1673–1677. [PubMed: 19556500]

Drury JL, Dennis RG, Mooney DJ. The tensile properties of alginate hydrogels. Biomaterials. 2004; 25:3187–3199. [PubMed: 14980414]

Ducheyne P, Qiu Q. Bioactive ceramics: the effect of surface reactivity on bone formation and bone cell function. Biomaterials. 1999; 20:2287–2303. [PubMed: 10614935]

Foppiano S, Marshall SJ, Marshall GW, Saiz E, Tomsia AP. The influence of novel bioactive glasses on in vitro osteoblast behavior. J Biomed Mater Res A. 2004; 71:242–249. [PubMed: 15372470]

Friedman CD, Costantino PD, Takagi S, Chow LC. BoneSource hydroxyapatite cement: a novel biomaterial for craniofacial skeletal tissue engineering and reconstruction. J Biomed Mater Res B. 1998; 43:428–432.

Gomes, ME.; Mikos, AG.; Reis, RL. Injectable Polymeric Scaffolds for Bone Tissue Engineering. In: Reis, RL.; San Roman, J., editors. Biodegradable Systems in Tissue Engineering and Regenerative Medicine. Boca Raton, FL, USA: CRC Press; 2004. p. 29-38.

Jäger M, Degistirici O, Knipper A, Fischer J, Sager M, Krauspe R. Bone healing and migration of cord blood-derived stem cells into a critical size femoral defect after xenotransplantation. J Bone Miner Res. 2007; 22:1224–1233. [PubMed: 17451370]

Jansen JA, Vehof JWM, Ruhe PQ, Kroeze-Deutman H, Kuboki Y, Takita H, Hedberg EL, Mikos AG. Growth factor-loaded scaffolds for bone engineering. J Controlled Release. 2005; 101:127–136.

Johnson PC, Mikos AG, Fisher JP, Jansen JA. Strategic directions in tissue engineering. Tissue Eng. 2007; 13:2827–2837. [PubMed: 18052823]

Kim K, Dean D, Mikos AG, Fisher JP. Effect of initial cell seeding density on early osteogenic signal expression of rat bone marrow stromal cells cultured on cross-linked poly(propylene fumarate) disks. Biomacromol. 2009; 10:1810–1817.

Kuo CK, Ma PX. Ionically crosslinked alginate hydrogels as scaffolds for tissue engineering: part I. Structure, gelation rate and mechanical properties. Biomaterials. 2001; 22:511–521. [PubMed: 11219714]

Laurencin CT, Ambrosio AMA, Borden MD, Cooper JA. Tissue engineering: Orthopedic applications. Annual Rev Biomed Eng. 1999; 1:19–46. [PubMed: 11701481]

Lavery K, Hawley S, Swain P, Rooney R, Falb D, Alaoui-Ismaili M. New insights into BMP-7 mediated osteoblastic differentiation of primary human mesenchymal stem cells. Bone. 2009; 45:27–41. [PubMed: 19306956]

Leach JK, Kaigler D, Wang Z, Krebsbach PH, Mooney DJ. Coating of VEGF-releasing scaffolds with bioactive glass for angiogenesis and bone regeneration. Biomaterials. 2006; 27:3249–3255. [PubMed: 16490250]

Link DP, van den Dolder J, van den Beucken JJ, Wolke JG, Mikos AG, Jansen JA. Bone response and mechanical strength of rabbit femoral defects filled with injectable CaP cements containing TGF-α1 loaded gelatin microspheres. Biomaterials. 2008; 29:675–682. [PubMed: 17996293]

Livak KJ, Schmittgen TD. Analysis of relative gene expression data using real-time quantitative PCR and the $2^{-\Delta\Delta Ct}$ Method. Methods. 2001; 25:402–408. [PubMed: 11846609]

Mao JJ, Giannobile WV, Helms JA, Hollister SJ, Krebsbach PH, Longaker MT, Shi S. Craniofacial tissue engineering by stem cells. J Dent Res. 2006; 85:966–979. [PubMed: 17062735]

Mao, JJ.; Vunjak-Novakovic, G.; Mikos, AG.; Atala, A. Regenerative medicine: Translational approaches and tissue engineering. Boston, MA, USA: Artech House; 2007.

Mikos AG, Herring SW, Ochareon P, Elisseeff J, Lu HH, Kandel R, Schoen FJ, Toner M, Mooney D, Atala A, Van Dyke ME, Kaplan D, Vunjak-Novakovic G. Engineering complex tissues. Tissue Eng. 2006; 12:3307–3339. [PubMed: 17518671]

Muzzarelli RAA, Biagini G, Bellardini M, Simonelli L, Castaldini C, Fraatto G. Osteoconduction exerted by methylpyrolidinone chitosan used in dental surgery. Biomaterials. 1993; 14:39–43. [PubMed: 8425023]

Nuttelman CR, Tripodi MC, Anseth KS. *In vitro* osteogenic differentiation of human mesenchymal stem cells photoencapsulated in PEG hydrogels. J Biomed Mater Res A. 2004; 68:773–782. [PubMed: 14986332]

Praemer, A.; Furner, S.; Rice, DP. Musculoskeletal conditions in the United States. Rosemont, Illinois, USA: Amer Acad Orthop Surg; 1999. chapter1

Radin S, Reilly G, Bhargave G, Leboy PS, Ducheyne P. Osteogenic effects of bioactive glass on bone marrow stromal cells. J Biomed Mater Res A. 2005; 73:21–29. [PubMed: 15693019]

Reilly GC, Radin S, Chen AT, Ducheyne P. Differential alkaline phosphatase responses of rat and human bone marrow derived mesenchymal stem cells to 45S5 bioactive glass. Biomaterials. 2007; 28:4091–4097. [PubMed: 17586040]

Salinas CN, Anseth KS. The influence of the RGD peptide motif and its contextual presentation in PEG gels on human mesenchymal stem cell viability. J Tissue Eng Regen Med. 2008; 2:296–304. [PubMed: 18512265]

Shi X, Sitharaman B, Pham QP, Liang F, Wu K, Billups EW, et al. Fabrication of porous ultra-short single-walled carbon nanotube nanocomposite scaffolds for bone tissue engineering. Biomaterials. 2007; 28:4078–4090. [PubMed: 17576009]

Shindo ML, Costantino PD, Friedman CD, Chow LC. Facial skeletal augmentation using hydroxyapatite cement. Arch Otolaryngol Head Neck Surg. 1993; 119:185–190. [PubMed: 8427682]

Sitharaman B, Shi X, Walboomers XF, Liao H, Cuijpers V, Wilson LJ, et al. *In vivo* biocompatibility of ultra-short single-walled carbon nanotube/biodegradable polymer nanocomposites for bone tissue engineering. Bone. 2008; 43:362–370. [PubMed: 18541467]

Sundelacruz S, Kaplan DL. Stem cell- and scaffold-based tissue engineering approaches to osteochondral regenerative medicine. Semin Cell Dev Biol. 2009; 20:646–655. [PubMed: 19508851]

Thein-Han WW, Saikhun J, Pholpramoo C, Misra RD, Kitiyanant Y. Chitosan-gelatin scaffolds for tissue engineering: physico-chemical properties and biological response of buffalo embryonic stem cells and transfectant of GFP-buffalo embryonic stem cells. Acta Biomaterials. 2009; 5:3453–3466.

Varghese S, Hwang NS, Ferran A, Hillel A, Theprungsirikul P, Canver AC, Zhang Z, Gearhart J, Elisseeff J. Engineering musculoskeletal tissues with human embryonic germ cell derivatives. Stem Cells. 2010; 28:765–774. [PubMed: 20178108]

Wang HS, Hung SC, Peng ST. Mesenchymal stem cells in the Wharton's jelly of the human umbilical cord. Stem Cells. 2004; 22:1330–1337. [PubMed: 15579650]

Wang L, Singh M, Bonewald LF, Detamore MS. Signalling strategies for osteogenic differentiation of human umbilical cord mesenchymal stromal cells for 3D bone tissue engineering. J Tissue Eng Regen Med. 2009; 3:398–404. [PubMed: 19434662]

Weiss ML, Medicetty S, Bledsoe AR, Rachakatla RS, Choi M, Merchav S, Luo Y, Rao MS, Velagaleti G, Troyer D. Human umbilical cord matrix stem cells: Preliminary characterization and effect of transplantation in a rodent model of Parkinson's disease. Stem Cells. 2006; 24:781–792. [PubMed: 16223852]

Xu HHK, Quinn JB, Takagi S, Chow LC. Synergistic reinforcement of in situ hardening calcium phosphate composite scaffold for bone tissue engineering. Biomaterials. 2004; 25:1029–1037. [PubMed: 14615168]

Xu HHK, Takagi S, Sun L, Hussain L, Chow LC, Guthrie WF, et al. Calcium phosphate cement with non-rigidity and strength durability for periodontal bone repair. J Am Dent Assoc. 2006; 137:1131–1138. [PubMed: 16873330]

Xu HHK, Carey LE, Burguera EF. Strong, macroporous, and in situ-setting calcium phosphate cement layered structures. Biomaterials. 2007; 28:3786–3796. [PubMed: 17574665]

Yao J, Radin S, Reilly G, Leboy PS, Ducheyne P. Solution-mediated effect of bioactive glass in poly (lactic-co-glycolic acid)-bioactive glass composites on osteogenesis of marrow stromal cells. J Biomed Mater Res A. 2005; 75:794–801. [PubMed: 16138322]

Zhao L, Weir MD, Xu HHK. An injectable calcium phosphate - alginate hydrogel - umbilical cord mesenchymal stem cell paste for bone tissue engineering. Biomaterials. 2010a; 31:6502–6510. [PubMed: 20570346]

Zhao L, Burguera EF, Xu HHK, Amin N, Ryou H, Arola DD. Fatigue and human umbilical cord stem cell seeding characteristics of calcium phosphate-chitosan-biodegradable fiber scaffolds. Biomaterials. 2010b; 31:840–847. [PubMed: 19850337]

Zhang ZY, Teoh SH, Chong MS, Schantz JT, Fisk NM, Choolani MA, et al. Superior osteogenic capacity for bone tissue engineering of fetal compared with perinatal and adult mesenchymal stem cells. Stem Cells. 2009; 27:126–137. [PubMed: 18832592]

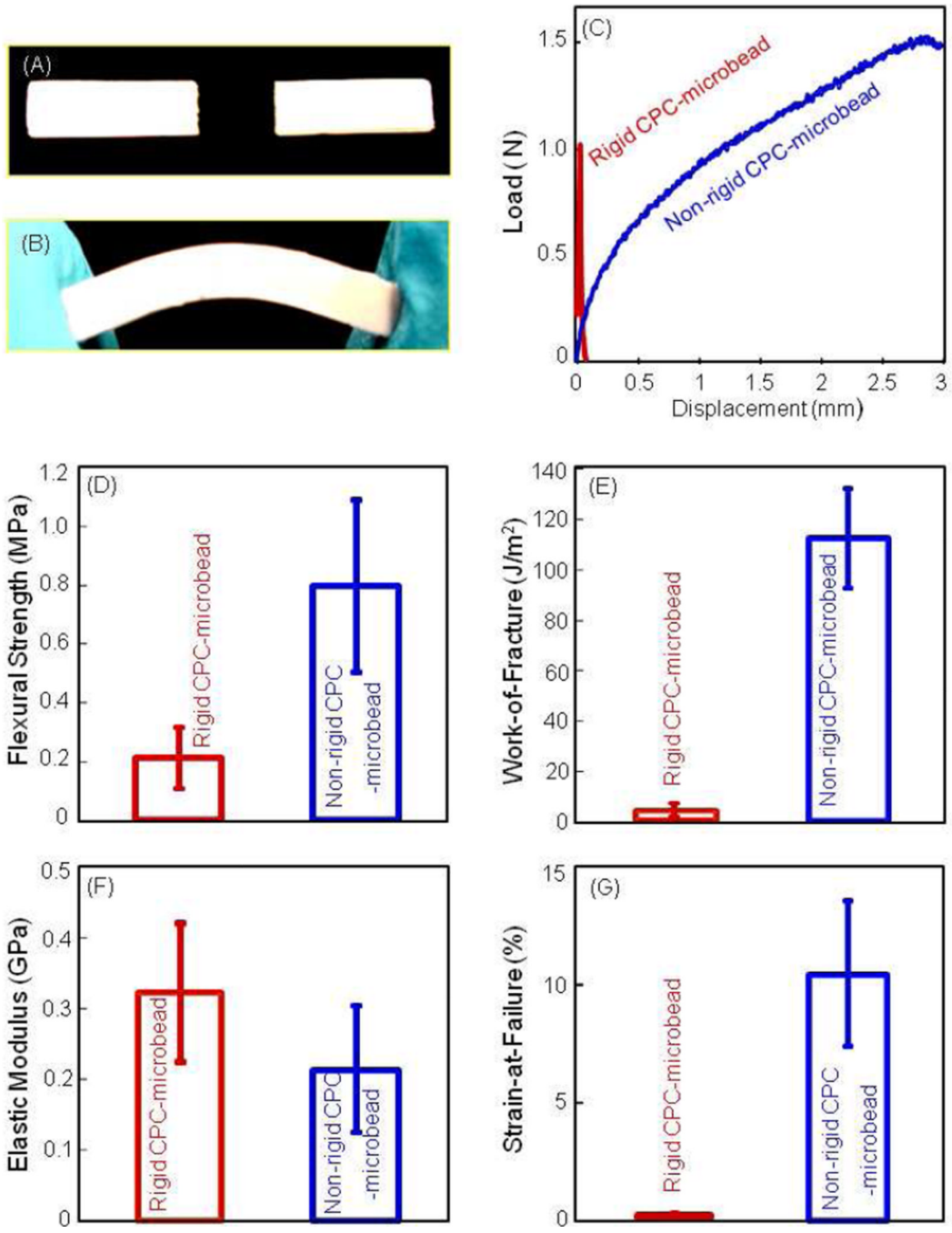


**Figure 1.**

Mechanical properties of the traditional rigid CPC and the new non-rigid CPC scaffold. (A) Rigid CPC fractured catastrophically. (B) The non-rigid CPC-microbead scaffold showed a brittle to tough transition. (C) Typical load-displacement curves. (D) Flexural strength, (E) work-of-fracture (toughness), (F) elastic modulus, and (G) strain-at-failure. Each value is the mean of five measurements with the error bar showing one standard deviation (mean ± sd; n = 5).

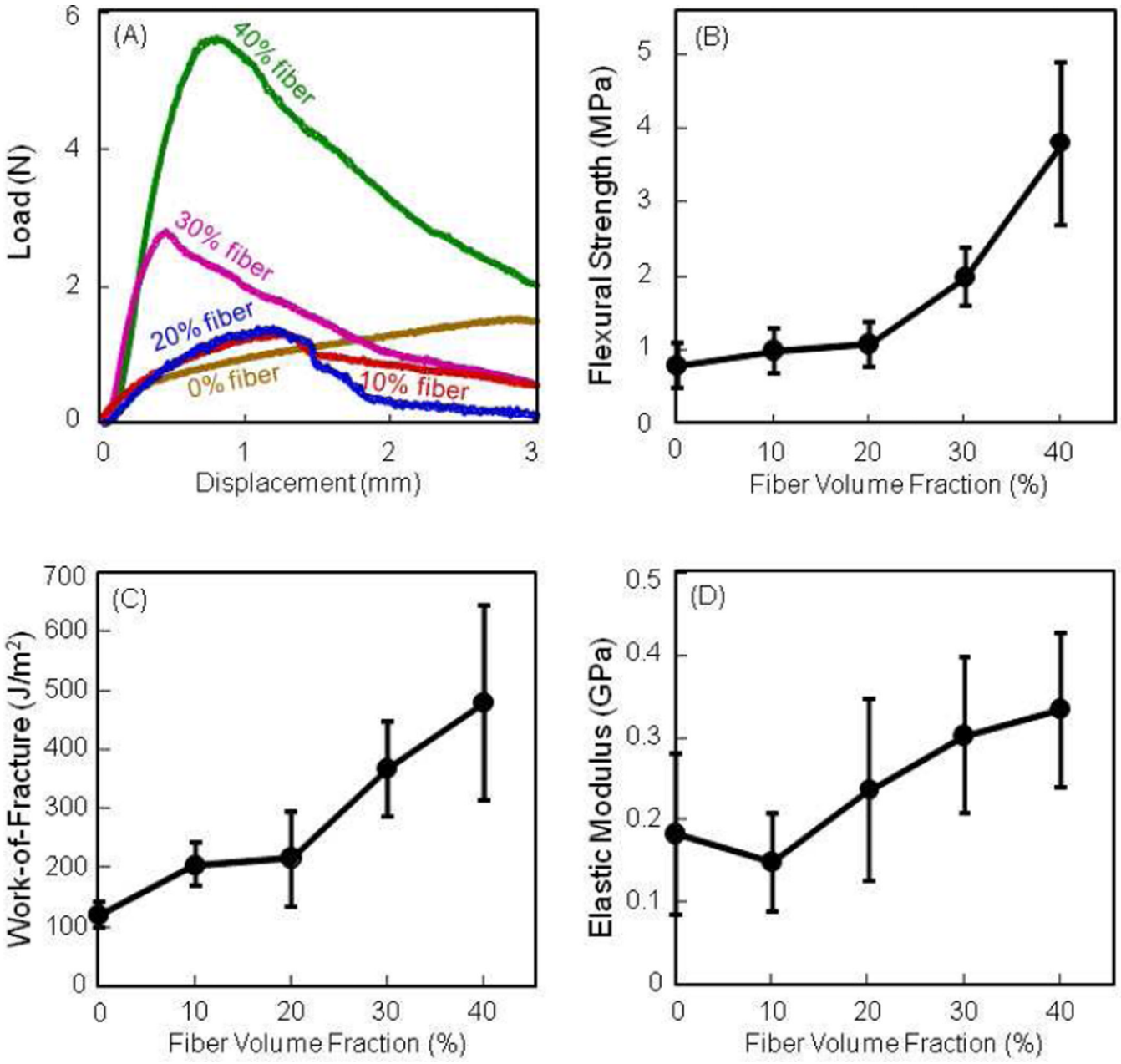


**Figure 2.**

Effect of fiber volume fraction on mechanical properties of non-rigid CPC-microbead scaffold. (A) Non-catastrophic failure of the fiber-reinforced non-rigid CPC scaffold. (B) Flexural strength, (C) work-of-fracture, and (D) elastic modulus. Each value is mean ± sd; n = 5.

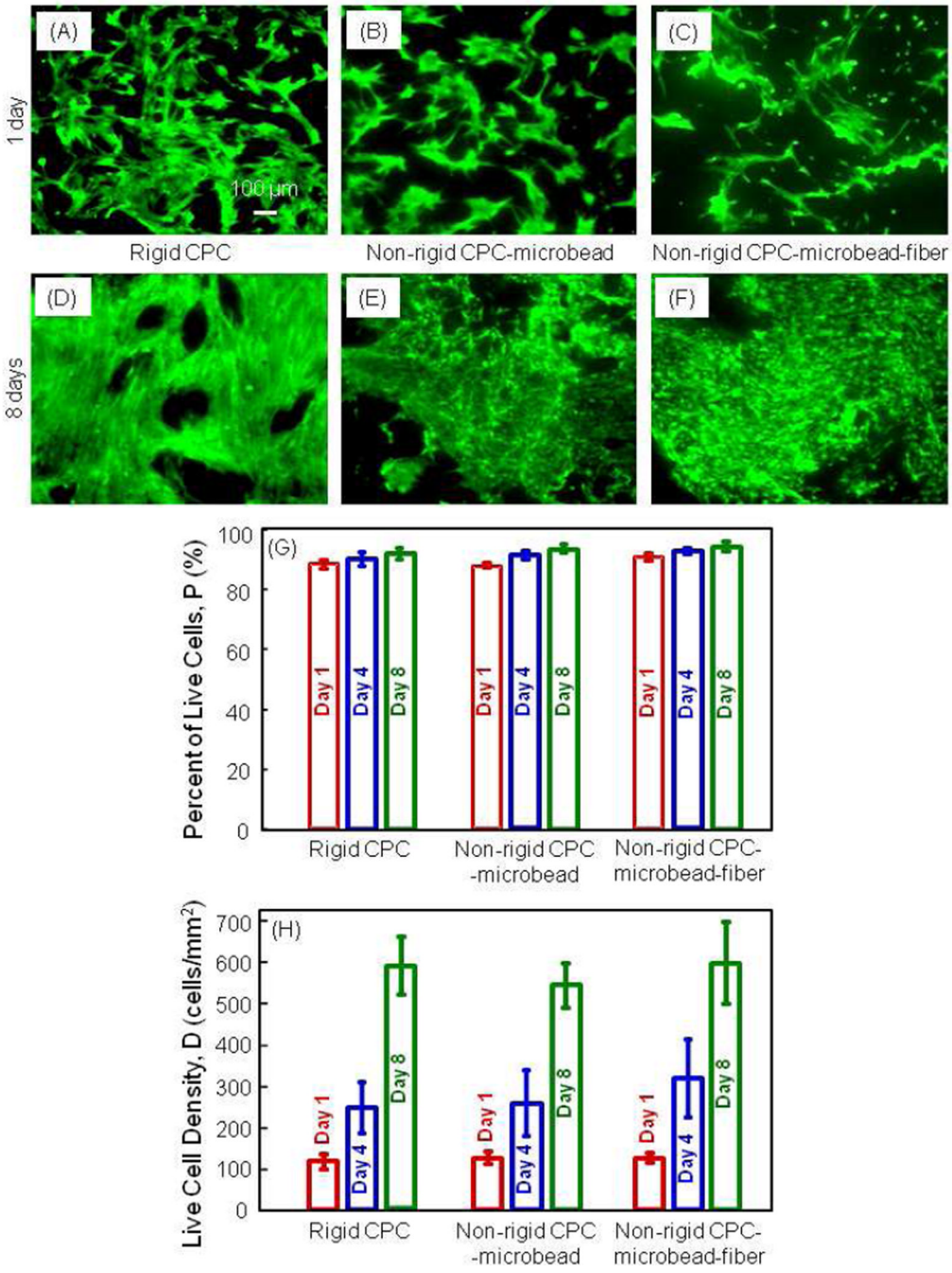


**Figure 3.**

Live/dead assay results of hUCMSCs on non-rigid CPC-microbead-fiber scaffold. (A–C) Live cells were stained green and were numerous on all materials. (D–F) hUCMSCs proliferated and increased in cell density by 8 d. (G) Percentage of live cells. (H) hUCMSCs proliferation, with cell density increasing by 5-6 fold in 7 d on all three constructs. Each value is mean ± sd; n = 5.

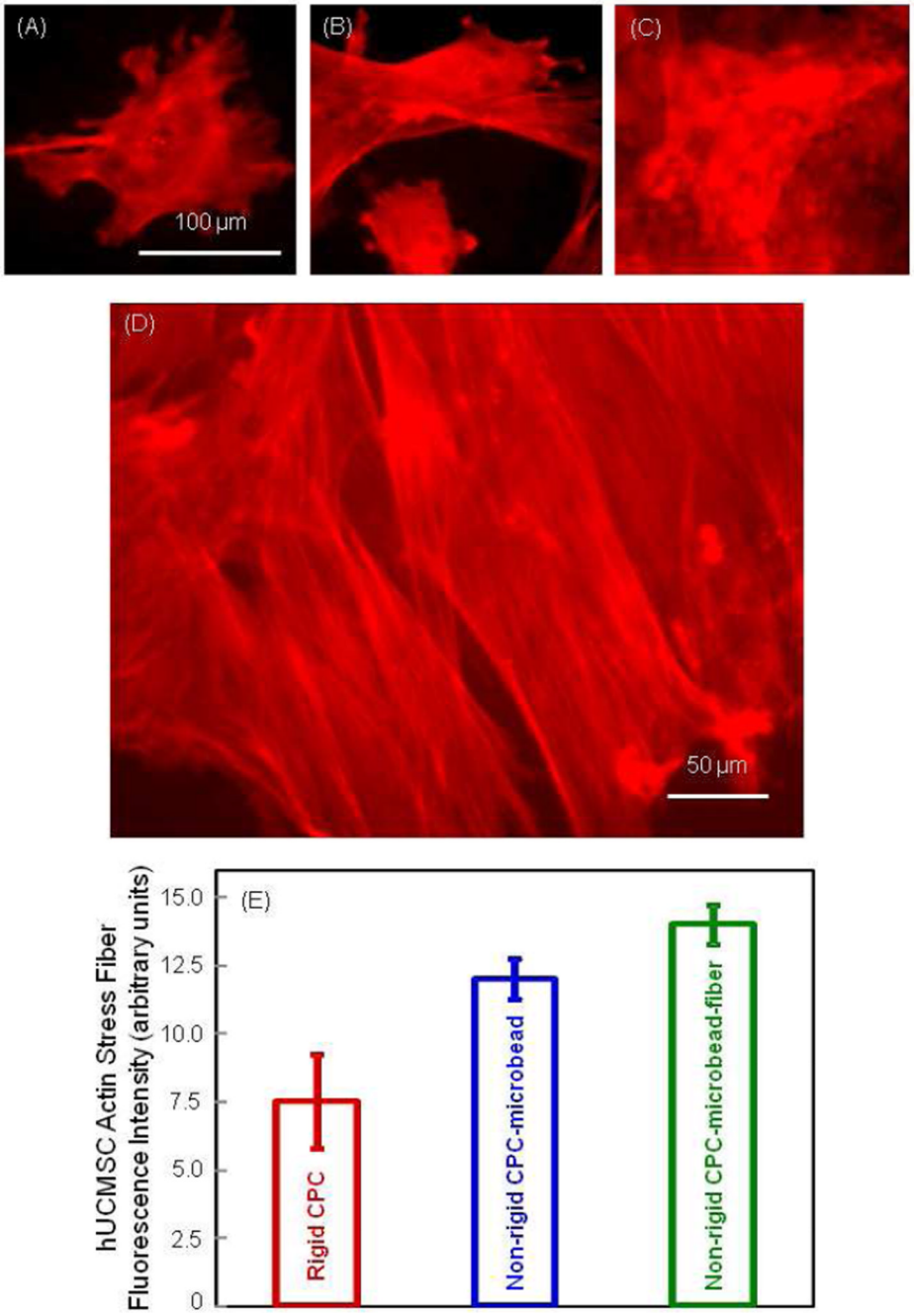


**Figure 4.**

Fluorescence of actin stress fibers inside the hUCMSCs adhering on the scaffolds. (A) Rigid CPC, (B) non-rigid CPC-microbead scaffold, and (C) non-rigid CPC-microbead-fiber scaffold. (D) Higher magnification showing examples of actin stress fibers. (E) Actin stress fiber fluorescence intensity (mean ± sd; n = 5). These three values are significantly different from each other ($p < 0.05$).

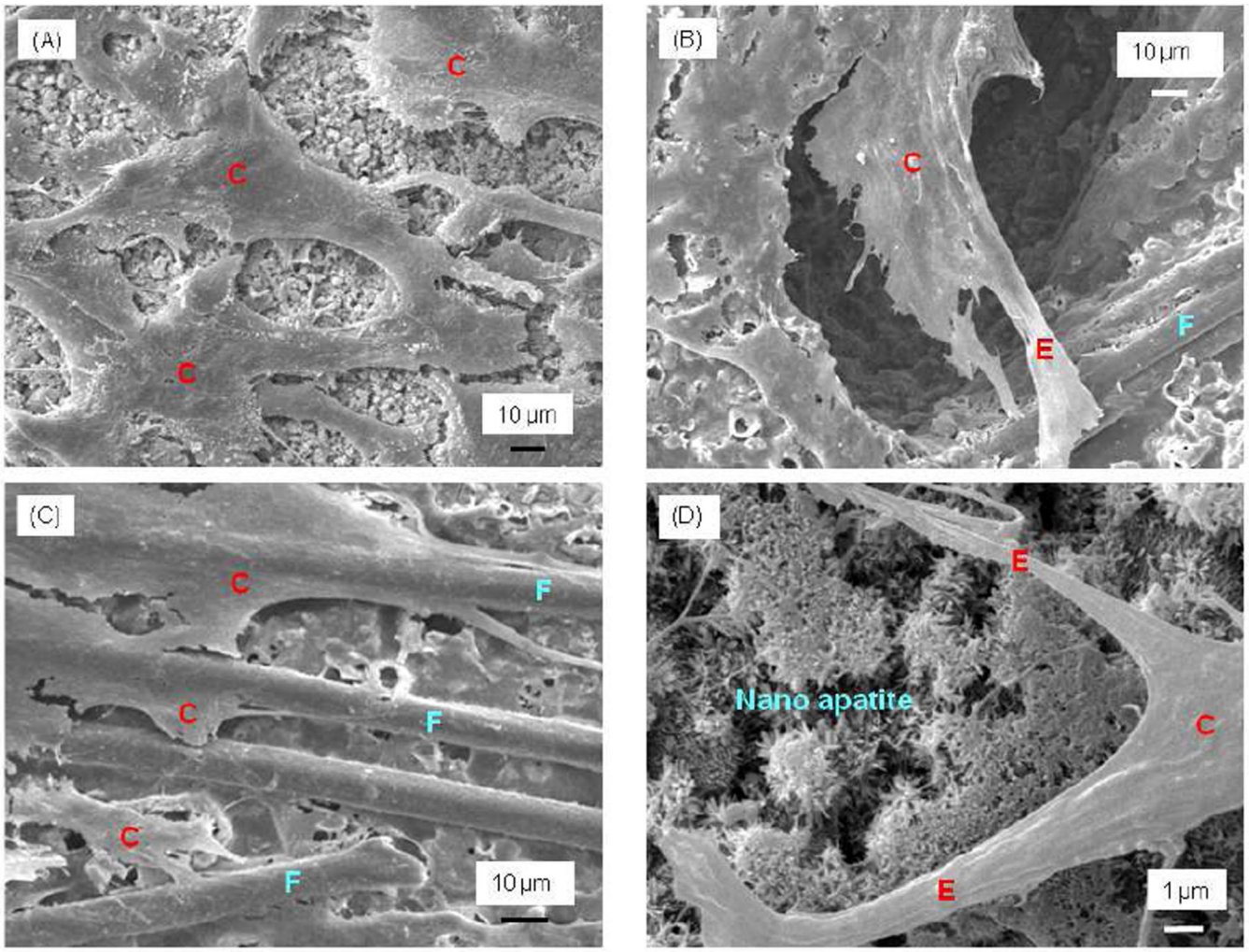


**Figure 5.**
SEM of hUCMSC attachment on scaffolds. (A) hUCMSC attachment on rigid CPC construct at 1 d. (B) and (C) hUCMSC anchorage and spreading on the non-rigid CPC-microbead-fiber construct. “C” refers to the hUCMSCs. Cells developed long cytoplasmic extensions “E” that anchored to the fibers “F”. (D) Higher magnification of cell attaching to the nano-apatite crystals in CPC. hUCMSCs attained a normal polygonal morphology.

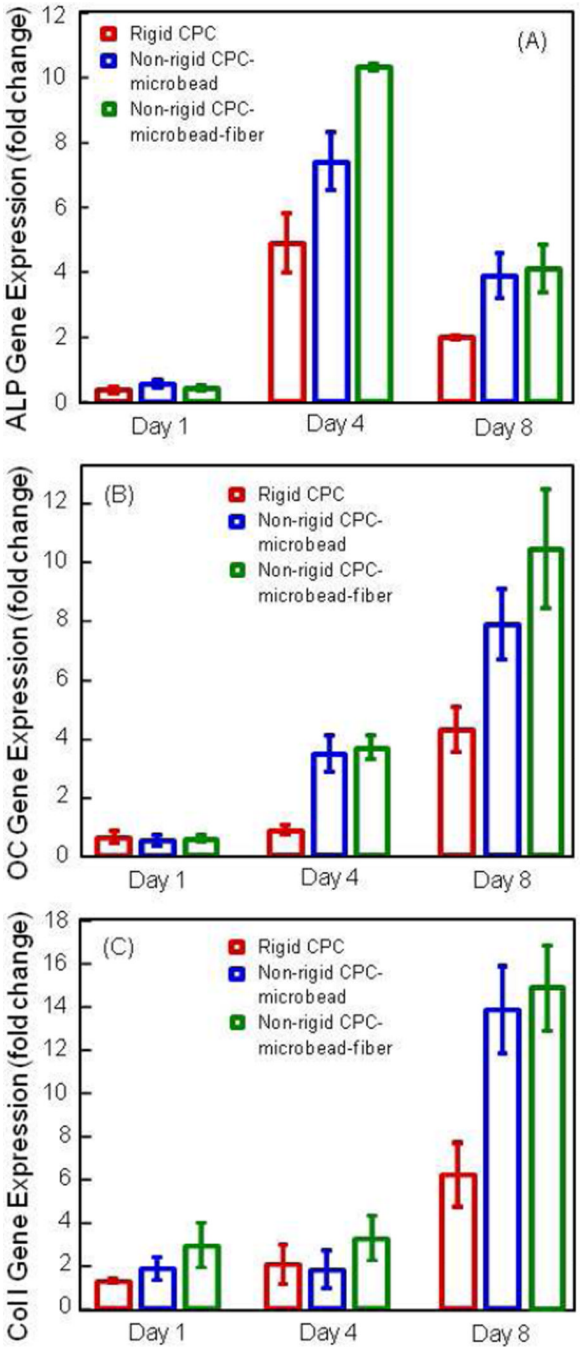


**Figure 6.**

Osteogenic differentiation of hUCMSCs. (A) Alkaline phosphatase activity (ALP) gene expression. (B) Osteocalcin (OC) expression. (C) Collagen type I expression. ALP was minimal at 1 d, peaked at 4 d, then decreased at 8 d. OC and collagen I peaked at 8 d. hUCMSCs on non-rigid CPC-microbead-fiber construct had higher ALP, OC and collagen I expressions than those on conventional rigid CPC. Each value is mean ± sd; n = 5.

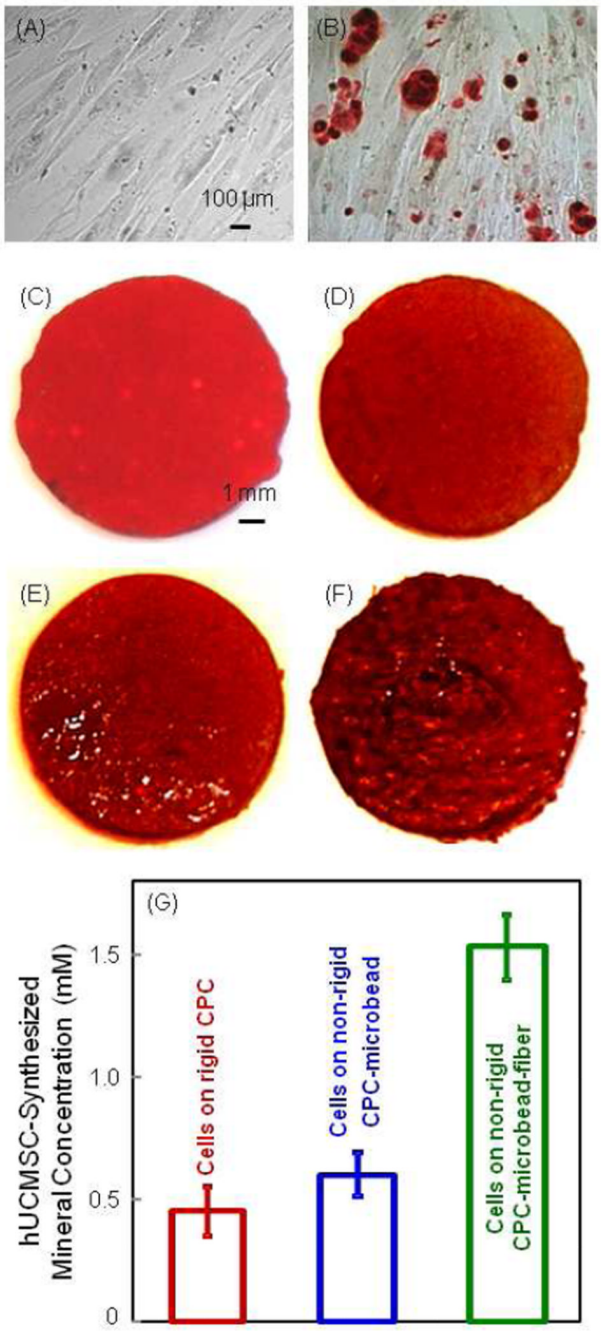


**Figure 7.**

Alizarin Red S (ARS) staining of bone mineralization by hUCMSCs. It stains calcium minerals into a red color. (A) hUCMSCs on TCPS in control media at 14 d. (B) hUCMSCs on TCPS in osteogenic media at 14 d. (C) CPC disk with no cells. (D) Rigid CPC, (E) nonrigid CPC-microbead scaffold, and (F) non-rigid CPC-microbead-fiber scaffold. D–F were seeded with hUCMSCs and cultured in osteogenic media for 14 d. (G) Mineral concentration measured via the osteogenesis assay (mean ± sd; n = 5). hUCMSCs synthesized more mineral on the non-rigid CPC-microbead-fiber scaffold than that of the other two constructs ($p < 0.05$).